CHINA SHIP SCIENTIFIC RESEARCH CENTER

AN INTEGRATED METHOD FOR COMPUTING THE INTERNAL AND EXTERNAL VISCOUS FLOW FIELD AROUND THE DUCTED PROPULSOR BEHIND AN AXISYMMETRIC BODY

Zhou Lian-di Zhao Feng

August 1994

CSSRC Report
English version 94004

P. O. BOX 116, WUXI, JIANGSU

CHINA

Contents

	page
Abstract	
Introduction	1
Governing equations and boundary condition	2
H-type boundary fitted grid system and semi-staggered grid	3
Difference discretization and the pressure solving equation in continuity formulation	3
Representation of the propeller	5
Numerical examples	5
case 1. flow over the body woth a duct	5
case 2. flow over the body with a duct and an operating propeller	5
case 3. flow over the accelerative ducted propeller	5
case 4. flow over a backstep stern fitted duct with rotor and stator	6
Conclusion	6
Acknowledgment	6
References	6

AN INTEGRATED METHOD FOR COMPUTING THE INTERNAL AND EXTERNAL VISCOUS FLOW FIELD AROUND THE DUCTED PROPULSOR BEHIND AN AXISYMMETRIC BODY

Zhou Lian-di and Zhao Feng
China Ship Scientific Research Center
P. O. Box 116, Wuxi 214082, Jiangsu, P. R. China

ABSTRACT

This paper presents an effective method for computing the internal and external viscous flow field around the ducted propulsor behind an axisymmetric body by using a new Navier-Stokes equations solver with primitive variable continuity equation formulation. In the present numerical method, the calculation equation for pressure with well-defined coefficient, which form is similar to the artificial compressibility method, is developed. A semi-staggered grid system is adopted. Not only the advantage of staggered grid system can be retrained but the boundary conditions on the inner and outer surface of the duct can be also carried out easily. By using a special grid system and the programming technique for implementing the jump boundary condition on the duct surfaces, the internal and external viscous flow field around the ducted propulsor behind the axisymmetric body may be calculated integrally in an unified numbered grid system. Some configurations are calculated and compared with experimental date and numerical results of other methods. Illustrative calculations are also presented for a stern of axisymmetric body with the backstep fitted a duct to illustrate the capability of the present method. Beside that, the effect of axial distribution of body force is considered and discussed in order to extend the application range of the present method.

INTRODUCTION

It has been known in marine propulsion technology that the use of ducted propeller has often been an attractive alternative for ship and underwater vehicle propulsion as well. With a duct that accelerates the flow, the propulsive efficiency can be increased. With a duct that decelerates the flow, the inception of cavitation on the propeller can be delayed. In order to take advantage of the ducted propeller to obtain the desirable benefit, a clear understanding of the role it plays is important. The reliable numerical simulation of the flow field around the ducted propeller is a useful tool to gain understanding. Various potential theories have been used to model ducted propulsors in uniform flow with varying degrees of success. For a submerged vehicle, the propulsor is operating within the thick boundary layer developed near the stern. The potential methods cannot take into account the interaction between the ducted propulsor and the strong vorticity field inside the boundary layer. Thus, it is necessary to use Navier-Stokes equations solver for analyzing the viscous flow field around the ducted propulsor/stern. When a ducted propulsor operates in the non-uniform wake of ship, the resulting flow field is that due to the hull, duct and propeller combination body. For this flow field, the exact treatment is to incorporate the actual propeller into a viscous flow calculation method and no-slip boundary condition must be satisfied on surfaces of the hull, duct and rotating blades of the propeller. However, it is still a very difficult problem today to solve the flow field of a hull, duct and propeller combination body by using such an exact method. The popular research work is that the body force field which presents the effect of propeller is incorporated into the Navier-Stokes equations. Beside that, another difficult problem raised due to the duct which divides the flow field into the internal and external flow field. In existed methods for computing the viscous flow field around the ducted propeller behind an axisymmetric body, the streamline-iteration method adopted by Schmiechen and Zhou [1] must know the flow rate entered the duct beforehand, and the multiblock iteration method employed by Yang et al [2] and Dai et al [3] will increase CPU time.

In the present paper an effective method for computing the internal and external viscous flow

field around the ducted propulsor behind an axisymmetric body is developed. In numerical method, the time-dependence Reynolds Average Navier-Stokes equation with primitive variable formulation is solved, k-ε two equation turbulence model is employed and the effect of the propeller inside the duct is modeled by a body force. There are three features in our numerical method. Firstly, by using the point relaxation method the continuity equation is transformed the calculation formula for the pressure, which has a formal resemblance to the formula of artificial compressibility method, but its coefficient is well-defined and depends on the geometric parameters of grid and the velocities in the neighborhood of the calculating points. Thus, the pressure adjustment is adapted to the neibouring flow field. The drawback of slow convergence for the pressure and residuum of the continuity equation in using the original artificial compressibility method, which is due to the inconsistency of artificial velocity of pressure wave propagation with the real physics, is overcome. Secondly, a semi-staggered grid system is developed, i.e. u, w, k, and ε are defined at the node of grid and v and p are defined on the usual staggered grid system. Therefore, not only the advantage of staggered grid system can be retrained but the boundary conditions on the inner and outer wall of the duct can be also easily carried out. Finally, by using a special grid system and the programming technique for implementing the jump boundary condition on the transformed duct wall, the internal and external viscous flow field around the ducted propulsor behind the axisymmetric body may be calculated integrally in an unified numbered grid system. Thus, two block iteration calculation between internal and external flow field inside and outside duct may be avoided and the computing time is saved. Three difference configurations are calculated and compare with experimental data and the numerical results of other methods. These are, 1.axisymmetric body with a duct, 2. axisymmetric body with a duct and an operating propeller, 3. accelerate ducted propeller. Illustrative calculation is also presented for a stern of axisymmetric body with the backstep fitted a duct to illustrate the capability of the present method, which can calculate a very full afterbody even with backstep. Beside that, the effect of axial distribution of body force is considered and discussed in order to extend the application range of the present method.

GOVERNING EQUATIONS AND BOUNDARY CONDITION

The nondimensional equations of axisymmetric viscous incompressible flow are written in cylindrical polar coordinates (x,r,θ) in the physical domain as follows:

$$\frac{\partial U}{\partial x}+\frac{1}{r}\frac{\partial}{\partial r}(rV)=0 \tag{1}$$

$$\frac{\partial U}{\partial t}+U\frac{\partial U}{\partial x}+V\frac{\partial U}{\partial r}+\frac{\partial}{\partial x}(p+\overline{uu})+\frac{\partial}{\partial r}(\overline{uv})+\frac{\overline{uv}}{r}-\frac{1}{Re}\nabla^2U=fb_x \tag{2}$$

$$\frac{\partial V}{\partial t}+U\frac{\partial V}{\partial x}+V\frac{\partial V}{\partial r}-\frac{W}{r}+\frac{\partial}{\partial x}(\overline{uv})+\frac{\partial}{\partial r}(p+\overline{vv})+\frac{\overline{vv}}{r}-\frac{\overline{ww}}{r}-\frac{1}{Re}(\nabla^2V+\frac{V}{r^2})=0 \tag{3}$$

$$\frac{\partial W}{\partial t}+U\frac{\partial W}{\partial x}+V\frac{\partial W}{\partial r}+\frac{WV}{r}+\frac{\partial}{\partial x}(\overline{uw})+\frac{\partial}{\partial r}\overline{vw}+2\frac{\overline{vw}}{r}-\frac{1}{Re}(\nabla^2W-\frac{W}{r^2})=fb_\theta \tag{4}$$

$$\frac{\partial k}{\partial t}+U\frac{\partial k}{\partial x}+V\frac{\partial k}{\partial r}=\frac{\partial}{\partial x}(\frac{1}{R_{eff}}\frac{\partial k}{\partial x})+\frac{1}{r}\frac{\partial}{\partial r}(\frac{1}{R_{eff}}r\frac{\partial k}{\partial r})+G-\varepsilon \tag{5}$$

$$\frac{\partial \varepsilon}{\partial t}+U\frac{\partial \varepsilon}{\partial x}+V\frac{\partial \varepsilon}{\partial r}=\frac{\partial}{\partial x}(\frac{1}{R_{eff}}\frac{\partial \varepsilon}{\partial x})+\frac{1}{r}\frac{\partial}{\partial r}(\frac{1}{R_{eff}}r\frac{\partial \varepsilon}{\partial r})+G_\varepsilon\frac{\varepsilon}{k}-C_{\varepsilon 2}\frac{\varepsilon^2}{k} \tag{6}$$

In above six equations U,V, and W is the mean velocity components in the (x,r,θ) coordinates system; p is the nondimensional pressure; $Re=\frac{U_\infty L}{\nu}$ is the Reynolds number defined in terms of characteristic velocity U_∞ , characteristic length L and molecular kinematic viscous ν ; k and ε are turbulent kinetic energy and its dissipation rate respectively; the barred quantities $\overline{uu}$, $\overline{uv}$ etc. are the Reynolds stresses normalized by U_∞^2 ; $\nu_t=\frac{C_\mu k^2}{\varepsilon}$ is the eddy viscosity; R_{eff} is the effective Reynolds number

$$R_{eff}=\frac{1}{R_e}+\frac{\nu_t}{\sigma_\phi} \tag{7}$$

where $\phi = k$ for the k-equation (5) and $\phi = \varepsilon$ for the ε-equation (6); G is the turbulence generation term.

$$G = \nu_t\left\{2\left[\left(\frac{\partial U}{\partial x}\right)^2 + \left(\frac{\partial V}{\partial r}\right)^2 + \left(\frac{V}{r}\right)^2\right] + \left(\frac{\partial U}{\partial r} + \frac{\partial V}{\partial x}\right)^2 + \left(\frac{\partial W}{\partial x}\right)^2 + \left(\frac{\partial W}{\partial r} - \frac{W}{r}\right)^2\right\} \quad (8)$$

In the two-equation k-ε turbulence model each Reynolds stress is related to the corresponding mean rate of strain by the isotropic eddy viscosity ν_t as follows:

$$\begin{cases} -\overline{uv} = \nu_t\left(\dfrac{\partial U}{\partial r} + \dfrac{\partial V}{\partial x}\right) \\ -\overline{uw} = \nu_t \dfrac{\partial W}{\partial x} \\ -\overline{vw} = \nu_t\left(\dfrac{\partial W}{\partial r} - \dfrac{W}{r}\right) \\ -\overline{uu} = \nu_t\left(2\dfrac{\partial U}{\partial x}\right) - \dfrac{2}{3}k \\ -\overline{vv} = \nu_t\left(2\dfrac{\partial V}{\partial r}\right) - \dfrac{2}{3}k \\ -\overline{ww} = \nu_t\left(2\dfrac{V}{r}\right) - \dfrac{2}{3}k \end{cases} \quad (9)$$

The model constants are:

$C_\mu = 0.09$, $C_{\varepsilon 1} = 1.44$, $C_{\varepsilon 2} = 1.92$, $\sigma_k = 1.0$, $\sigma_\varepsilon = 1.3$

The above equations (1) - (9) form a set of closed solving equations. For the axisymmetrical internal and external flow as shown in the figure 1., the boundary conditions are as follows:

Inlet: $V = W = 0$, $k = 0.00375U_\infty^2$, $\varepsilon = k^{1.5}/2$, U is determined according to the boundary layer thickness of flat plate and 1/7 rule;

Exit: $\dfrac{\partial U}{\partial x} = \dfrac{\partial V}{\partial x} = \dfrac{\partial W}{\partial x} = \dfrac{\partial k}{\partial x} = \dfrac{\partial \varepsilon}{\partial x} = 0$

Solid surface: $U = V = W = 0$, $\partial k/\partial n = 0$, ε is determined by the wall function.

Outer boundary: $U = 1$, $V = W = 0$, $\dfrac{\partial k}{\partial n} = \dfrac{\partial \varepsilon}{\partial n} = 0$

Wake centerline: $W = V = 0$, $\dfrac{\partial U}{\partial n} = \dfrac{\partial k}{\partial n} = \dfrac{\partial \varepsilon}{\partial n} = 0$

H-TYPE BOUNDARY FITTED GRID SYSTEM AND SEMI-STAGGERED GRID

The current method of elliptic boundary fitted grid generation [4] has been rather ripe, but the relations between the choice of the grid type and the practical physical problem are lesser considered. In the present method H-type grid is selected. It has the advantages that the form of the grid, boundary and relatively location in the calculation domain are coincident with those in the physical domain. This is specially suitable to the present internal and external flow problem. However, it is difficult to generate the good quantitative grid for H-type grid by using single block method. Therefore, the multiblock grid generation method [5] is used. The sketch of multiblock grid region is shown in Fig.1. For this multiblock grid, by using the programming technique for implementing the jump boundary condition on the both side of transformed duct surface and for properly taking boundary data in calculating the inner points near the both side of duct surface, the flow field of multiblock H-type grid which corresponds to the internal and external flow field around the duct can be solved in single block grid system. Thus, multiblock iteration between internal and external flow field inside and outside duct may be avoided and the CPU time is saved.

To overcome the difficulty of implementing boundary conditions in the staggered grid system; and at the same time to keep the advantages of the staggered grid, the equations are discretized in the semi-staggered grid system, i.e. U, W ,k, and ε are defined at the normal grid nodes, V and p are defined at the original staggered grid nodes, as shown in Fig.2. Thus the original advantage of the staggered grid can be retrained. The solving pressure is related to the neighbouring nodes and the pressure oscillation can be efficiently controlled. The boundary conditions on the inner and outer wall of the duct can be also easily carried out. Discreted difference equations are written on the grid of U,V,W,p,k and ε, respectively.

DIFFERENCE DISCRETIZATION AND THE PRESSURE SOLVING EQUATION IN CONTINUITY FORMULATION

Firstly,the governing equations (1) - (9) are transformed into the boundary fitted grid systems. The discretization methods and forms for the five equations are the same. The up-wind discretization scheme is used in the convection terms in order to keep the stability. For an example, the U equation is written as:

$$\frac{U^{n+1} - U^{n-1}}{2\Delta t} + AuU^{n+1} + BuP^{n+1} = 0 \quad (10)$$

where the superscripts n+1 and n-1 represent the value at n+1 and n-1 time step, respectively, Δt is the time step, Au and Bu are coefficient matries after discretization.

We calculate the middle time layer value to obtain:

$$\frac{U^* - U^{n-1}}{2\Delta t} + AuU^* + BuP^n = 0 \qquad (11)$$

where U^* represents value of U^{n+1} at the middle time layer. By using point relaxation method for the equation (11), we have

$$U^{*(k+1)} = U^{*(k)} + \omega\left[\frac{1}{2\Delta t} I + A_u^0\right]^{-1} \cdot \left[-A_u^- U^{*(k+1)} - A_u^0 U^{*(k)} - A_u^+ U^{*(k)} - BuP^n - \frac{1}{2\Delta t}(U^{*(k)} - U^{n-1})\right]$$
$$= U^{*(k)} + \omega\left[\frac{1}{2\Delta t} I + A_u^0\right]^{-1} \cdot rmu \qquad (12)$$

where $U^{*(k)}$ represents the k times iteration value of n+1 step at the middle layer; ω is the relaxation factor;

rmu is the difference remainder of the U momentum equation,

$$rmu = -A_u^- U^{*(k+1)} - A_u^0 U^{*(k)} - A_u^+ U^{*(k)} - BuP^n - \frac{1}{2\Delta t}(U^{*(k)} - U^{n-1}) \qquad (13)$$

A_u^- and A_u^+ are the lower-triangular matrix and the upper-triangular matrix of Au respectively, A_u^0 is the diagonal matrix of Au, I is unit diagonal matrix.

The discretization method and form of the V equation is similar to the above U equation, and the continuity equation is discretized as :

$$CuU^{n+1} + CvV^{n+1} = 0 \qquad (14)$$

where Cu and Cv are the coefficient matrices.

The pressure equation is derived as follows by substituting U^{n+1} and V^{n+1} into the discretized form of the continuity equation (14)

$$\omega\left\{\left[\frac{1}{2\Delta t} I + A_u^0\right]^{-1} \cdot CuBu + \left[\frac{1}{2\Delta t} I + A_v^0\right]^{-1} \cdot CvBv\right\} P^{n+1}$$
$$= Cu\left\{U^{n+1(k)} + \omega\left[\frac{1}{2\Delta t} I + A_u^0\right]^{-1} \cdot \left[-A_u^- U^{n+1(k+1)} - A_u^0 U^{n+1(k)} - A_u^+ U^{n+1(k)} - \frac{1}{2\Delta t}(U^{n+1(k)} - U^{n-1})\right]\right\}$$
$$+Cv\left\{V^{n+1(k)} + \omega\left[\frac{1}{2\Delta t} I + A_v^0\right]^{-1} \cdot \left[-A_v^- V^{n+1(k+1)} - A_v^0 V^{n+1(k)} - A_v^+ V^{n+1(k)} - \frac{1}{2\Delta t}(V^{n+1(k)} - V^{n-1})\right]\right\} \qquad (15)$$

Let us denote D as the coefficient matrix:

$$D = \omega\left\{\left[\frac{1}{2\Delta t} I + A_u^0\right]^{-1} Cu \cdot Bu + \left[\frac{1}{2\Delta t} I + A_v^0\right]^{-1} Cv \cdot Bv\right\} \qquad (16)$$

The equation (14) can be solved by point relaxation method. The initial value is assumed to be p^n and U^*,and V^* calculated by p^n. The equation (15) is written as the following simple form

$$P^{n+1} = p^n - \frac{r_p}{D_p} \nabla \cdot \vec{V}^* \qquad (17)$$

where D_p are the diagonal elements of the matrix D; r_p is the pressure relaxation factor for the pressure.

The form of equation (16) is similar to the artificial compressibility method[6] and relaxation coefficient r_p is easily chosen. Because D_p has defined value, which is related to geometric parameters of the grid and the velocities at the neighbouring grid nodes, thus, the pressure adjustment is adapted to the neighbouring flow field. The drawback of slow convergence for the pressure and residuum of the continuity equation in using original artificial compressibility method, which is due to the inconsistency of artificial velocity of pressure wave propagation with the real physics, is overcome. Comparing SIMPLE method, the solution of a Possion equation can be avoid and the CPU time can be decreased.

The coefficients of above discretization have been strictly derived under the semi-staggered grid system in the references [7].

REPRESENTATION OF THE PROPELLER

As mentioned in the introduction, the popular research work on the hull-propeller interaction is the body force field presentation of the propeller. In this method, the effect of the propeller is accounted for by the addition of body force terms in the source functions of Navier-Stokes equations. The essential parameters that defined the propeller effects are the thrust coefficient C_T, the torque coefficient C_Q, the advance coefficient J and the radial circulation distribution G(r). The same parameters are used to define the body force for the propeller model. The axial and circumferential body force per unit volume are obtained from the following equations:

$$fb_x = C_T R_p^2 G(r)/4\Delta x \int_{Rh}^{Rp} G(r)rdr ,$$
$$fb_\theta = C_Q R_p^3 G(r)/2r\Delta x \int_{Rh}^{Rp} G(r)rdr \qquad (18)$$

where R_h and R_p are the radii of propellor hub and blade tip respectively, and Δx is the thickness. Owing to the fact that, the blade circulation distribution depends upon the inflow at the propeller plane which in turn is influenced by the blade circulation. This mutual dependence implies that the body force fb_x and fb_θ which are functions of G(r) should be obtained by an iterative procedure. To complete this procedure, any propeller program can be used for this purpose.

If the discreted radial distributions for thrust and torque, $T(r_j)$ and $Q(r_j)$ j = 1,··· n, are known , From the formula

$$T = 2\pi\rho L^2 U_\infty^2 \Delta x \int_{Rh}^{Rp} fb_x(r)rdr$$
$$Q = 2\pi\rho L^3 U_\infty^2 \Delta x \int_{Rh}^{Rp} fb_\theta(r)r^2dr \qquad (19)$$

The body force field can be obtained as follows

$$fb_x(r_j^*) = \frac{T(r_j)}{2\pi\Delta x\rho L^2 U_\infty^2 r_j^*(r_{j+1} - r_j)}$$
$$fb_\theta(r_j^*) = \frac{\theta(r_j)}{2\pi\Delta x\rho L^3 U_\infty^2 r_j^{*2}(r_{j+1} - r_j)} \qquad (20)$$

where $r_j^* = 0.5(r_j + r_{j+1})$. Of course, to determine $T(r_j)$ and $Q(r_j)$ also needs an iterative procedure.

The iterative procedure is follow as:

(1) The flow field around the stern of and axisymmetric body only with a duct is calculated, and the inflow of the propeller may be obtained.

(2) The propeller performance calculation is carried out under the calculated inflow condition. The dimensionless circulation distribution G(r) or the thrust and torque distributions T(r) and Q(r) may be calculated and consequently the body force distributions $fb_x(r)$ and $fb_\theta(r)$ may be obtained.

(3) The flow field around the stern of an axisymmetric body with a duct and the body force field is calculated, and by substracting the propeller induced velocity from the calculated total velocity and the new inflow of the propeller may be obtained.

(4) Repeat calculations of step (2) to step (3) until the convergence is reached.

NUMERICAL EXAMPLES

The four configurations that were calculated are 1. flow over the body with a duct, 2. flow over the body with a duct and an operating propeller, 3. flow over an accelerative ducted propeller and 4. flow over a stern of axisymmetric body with the backstep fitted a duct with rotor and stator. The calculated results are compared with available experimental data and the numerical results of other methods.

case 1. Flow over the Body with a Duct

This numerical example is taken from [2]. Figure 3 shows the calculated velocity vectors in the stern region by the present method. Figure 4 shows the results from both computation of Yang's method and experiment[2].

case 2. Flow over the Body with a Duct and an Operating propeller

This numerical example is also taken from [2]. In this case the circulation G(r) and consequently the body force was assumed to be given. Figure 5 shows the calculated velocity vectors in the stern region by the present method. Figure 6 shows the results from both computation of Yang's method and experiment[2]. Comparing the above figures it can be seen that the essential flow phenomena such as separation, acceleration and contraction can be realistically predicted by the present method.

case 3. Flow over the Accelerative Ducted Propeller

This numerical example is the ducted propeller combined duct BD18 with propeller 6510. It was tested[9] and calculated by full-panel method[10] at CSSRC. In this example the viscous flow approach to the computation of hull-propeller interaction is carried out and the panel method developed by Xing[10] is used in computing propeller. Figure 7 shows the calculated velocity vector field around the duct. Figure 8 shows the calculated velocity profiles at the various axial locations for the flow over the duct without propeller and the comparison with the calculated results of the panel method[10]. Figure 9 and Figure 10 show the convergence procedure of the interactive iteration in computing the radial distributions of thrust and torque respectively. Table 1 shows the convergence procedure of the interactive iteration in computing the propeller performance characteristics and the comparison with the experiment and the calculated result of the full panel method. The agreement is satisfactory.

Table 1

performance / iteration number	K_T	$10K_Q$
1	0.2137	0.340
2	0.1353	0.235
3	0.1570	0.265
4	0.1498	0.255
5	0.1522	0.259
experiment[9]	0.1612	0.286
full panel method[10]	0.159	0.297

case 4. Flow over a Backstep Stern Fitted Duct with Rotor and Stator

This case is an illustrative calculation to illustrate the capability of the present method. The configuration is a stern of axisymmetric body with the backstep fitted a duct with rotor and stator. Figure 11 shows the calculated flow field around this configuration. The calculations are also carried out for two forms of axial distribution of body force shown in Figure 12. Figure 13 shows the calculated velocity profiles for these two forms of axial distribution of body force. From the above figures it can be seen that the essential phenomena such as separation, vorticity, deceleration and contraction can be realistically predicted and the influence of the axial distribution form of body force can be responded.

CONCLUSION

A numerical method based on the H-type boundary fitted grid system, semi-staggered grid discretization and the new calculation equation for pressure was developed. Numerical results indicate that this numerical method is effective and is specially suitable to solve the internal and external flow field problem. In order to extend the availability of the present method the effects of the appendage and strut should be incorporated in the further research work.

ACKNOWLEDGMENT

The authors would like to express their thank to Ms. Xing,W.P. for her help is carrying out the hull-propeller interaction calculation.

REFERENCES

[1] Schmiechen M. and Zhou,L. D., " An Advanced Method for Design of Optimal Ducted Propeller behind Bodies of Revolution", Proc. of SNAME Spring Meeting, Pittsburgh, 1988.

[2] Yang, C.I., Hartwich, P. and Sundaram, P., "A Navier-Stokes Solution of Hull-Ring Wing-Thruster Interaction", 18th ONR Symposium on Naval Hydrodynamics,1990

[3] Dai, M.H., Gorski, J.J. and Haussling, H.J., "Computation of an Integrated Ducted Propulsor/Stern Performance in Axisymmetric Flow.", Proc. of Propellers/Shafting '91 Symposium, Virginia, Sep. 17-18, 1991

[4] Thompson,J.F., "Numerical Grid Generation", Morth Holland, N.Y.,1982

[5] Zhao, F. and Zhou,L. D.,"A Coupled Generation Method for the General Three-Dimensional Multi-Block Grid", to be presented at Journal of Hydrodynamics.

[6] Chorin, A. J., " A Numerical Method for Solving Incompressible Viscous Flow Problems", Journal of Computational Physics, Vol.2 (1967), pp12-26

[7] Zhao, F. and Zhou,L.D., "The Flow Field Calculation around the Pump Jet", CSSRC Report,1993

[8] Stern, F., Kim, H.T., Patel, V.C. and Chen, H.C., "A Viscous Flow Approach to the Computation of Propeller-Hull Interaction", Journal of Ship Research, Vol. 32, No. 4, Dec. pp246-262, 1988

[9] Ye, Y. P., China Ship Scientific Research Center, Private Communication, April, 1994

[10] Xing, W. P., " Iteration Calculation in Panel Method for Performance Prediction of Multi-Body Flow.", CSSRC Report 1993

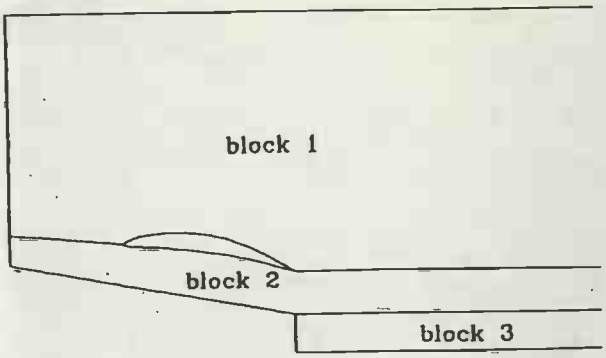

Fig. 1 Multi-Block Grid Region

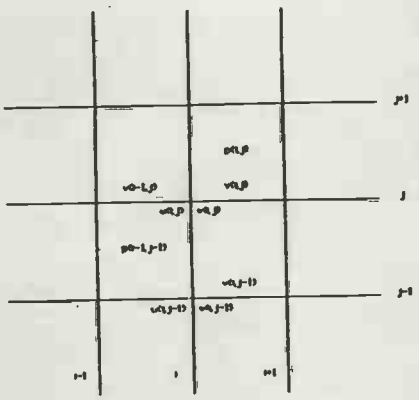

Fig. 2 Semi-Staggered Grid System

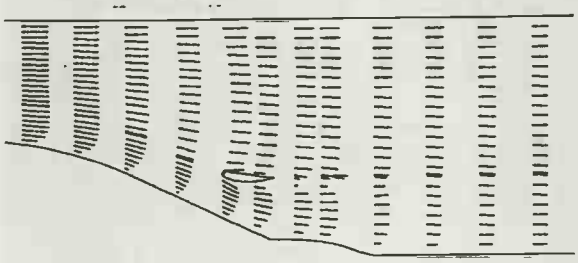

Fig. 3 Calculated Flow Field for Case 1

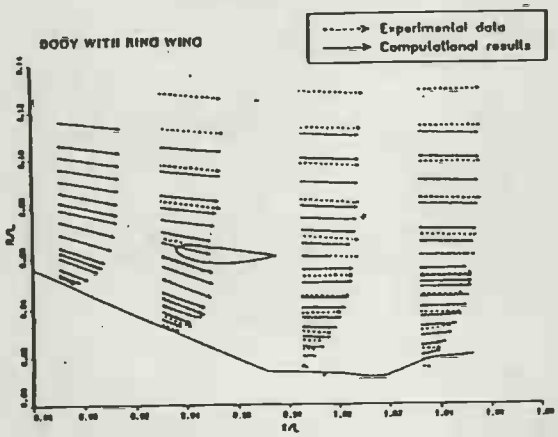

Fig. 4 Velocity Vectors in Stern Region for Case 1
(Experiment and Yang's Method)

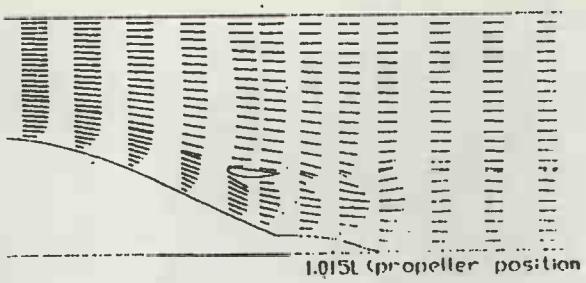

Fig. 5 Calculated Flow Field for Case 2

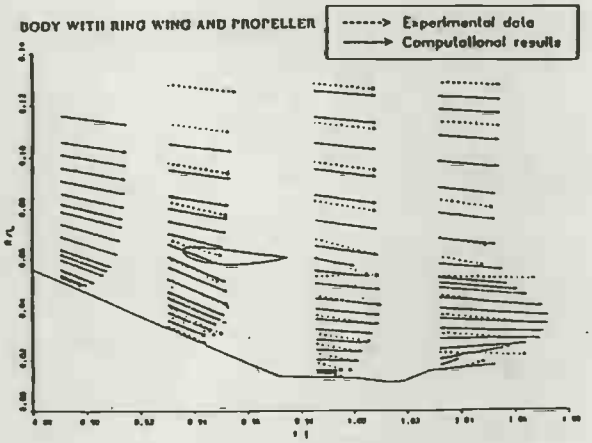

Fig. 6 Velocity Vectors in Stern Region for Case2
(Experiment and Yang's Method)

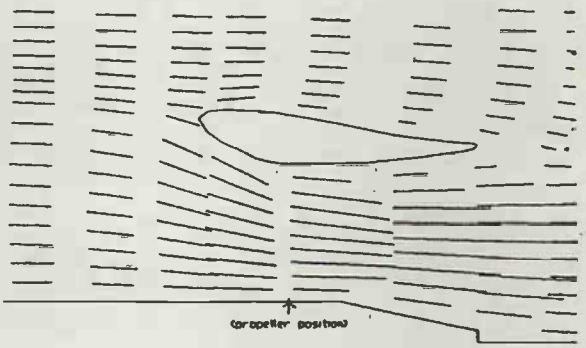

Fig. 7 Calculated Flow Field for Case 3

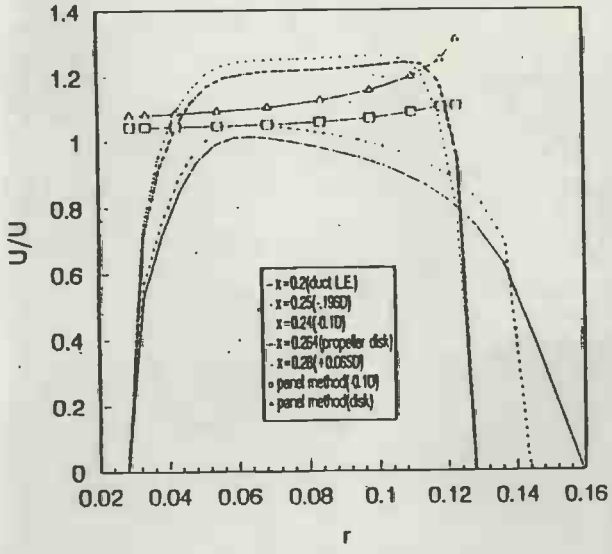

Fig. 8 Normal Wake of Duct BD18

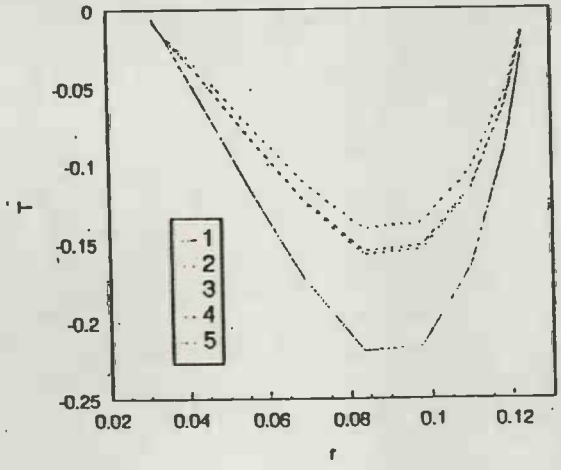

Fig. 9 Thrust Distribution for Propeller 6510 in Duct BD18

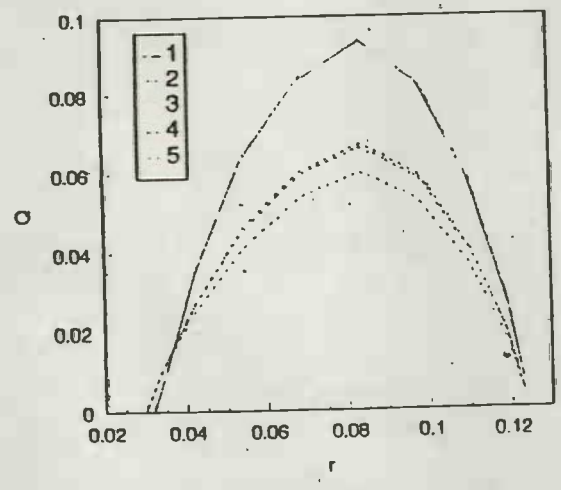

Fig. 10 Torque Distribution for Propeller 6510 in Duct BD18

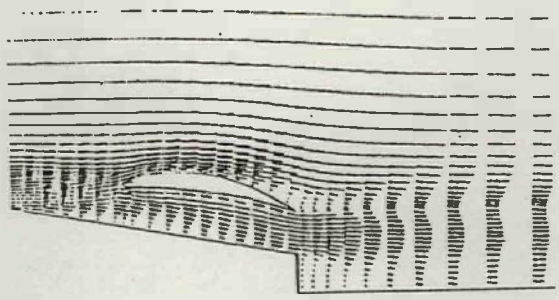

Fig 11. Calculated Flow Field For the Axisymmetric Body with a Backstep Stern Fitted a Duct

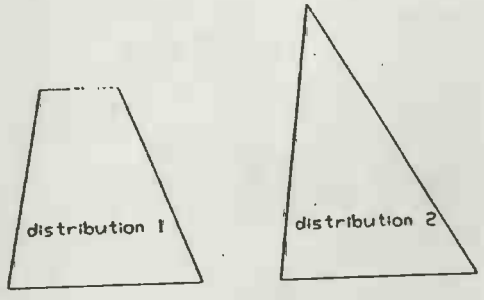

Fig. 12 Two Kind Axial Distribution Forms of Body Force Field

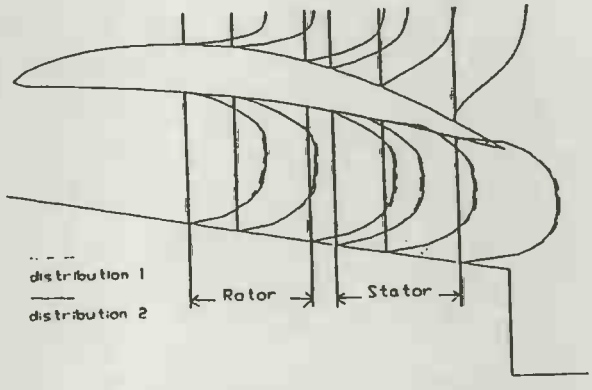

Fig. 13 Calculated Velocity Profiles for Two Axial Distribution Forms of Body Force Field